2008

The Biomechanics of Ballistochory in Impatiens Pallida

Lua Del Campo
Pomona College

The Biomechanics of Ballistochory in *Impatiens pallida*

Lua Del Campo
Advisor: Dr. Dwight Whitaker

September 19, 2008
Pomona College Department of Physics and Astronomy

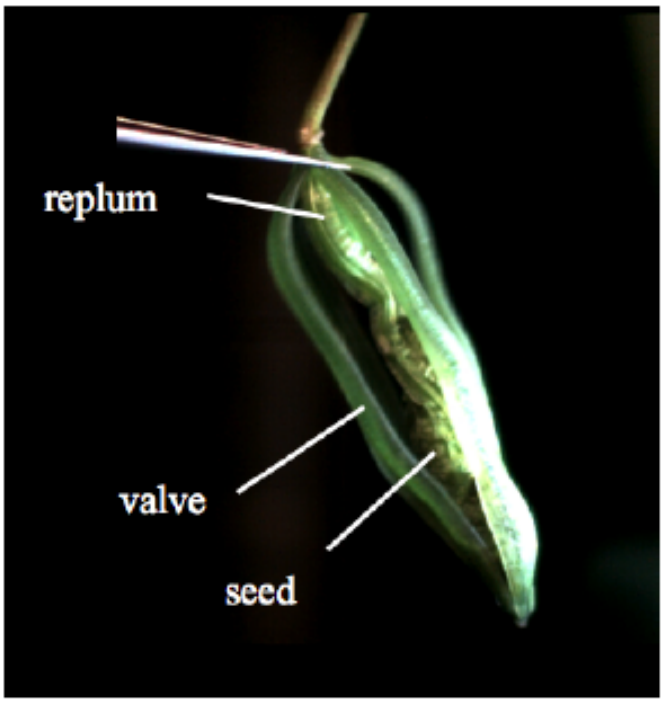

Contents

Abstract

This research is an analysis of the explosive seed dispersal of *Impatiens pallida* fruit. Data was taken using high-speed video and analyzed using LoggerPro video analysis software. From the videos we discerned a qualitative model for dehiscence, a description of how the process unfolds, and from our data we deduced quantitative values for the velocity, momentum, and energy of the system. We were also able to glean a lower bound of Young's modulus E of the fruit tissue. These results and the tools of analysis that generate them are the foundation for the development of a theoretical model of the plants motion. Our results also provide insights into *Impatiens pallida*'s evolutionary history by explaining its seed dispersal mechanism.

A secondary benefit of this research is providing ecologist's with new tools to analyze ultra-rapid movements in plants and fungi. These tools of analysis will assist in defining a plant's or fungi's evolutionary context and the ecological significance rapid motion plays.

Chapter 1

Plant Movement

1.1 Introduction

This undergraduate thesis is a study in biophysics. We will research how the plant *Impatiens pallida* physically interacts with its environment. Specifically we will research the physical processes involved in *I. pallida's* intrinsic seed-launching mechanism. Before we discuss our findings we will give an overview plant movement. A broader understanding of plant motion will help us place *Impatiens pallida*'s movement into context and demonstrate the significance of this study in the field of plant movement research.

1.2 Types of Plant Movement

There are many distinct forms and uses for movement in the plant and fungal kingdoms. Some well known examples are the rotation of a sunflower throughout the course of a day, or the closing of a Venus flytrap as a form of predation. Less commonly known are plants such as *Cornus canadensis*, which has exploding flowers that catapult pollen at a velocity of 6 m/s in under 0.5 ms [20], and the Sandbox Tree, *Hura crepitans*, that disperses its seeds at up to 70 m/s [16].

All plant movements can be placed in one of two categories, 1.) Movement that is governed by hydraulics and, 2.) Movement that results from released elastic potential energy. Movements that are founded in hydraulics, such as the motion of a sunflower, come about by the importing and exporting of fluid from the plant's cells. The cell wall, a feature unique to plant and fungal cells allows them to sustain an internal or turgor pressure of up to 10^6 N/m^2 [16]. Hydraulic movements are the result of the regulation of turgor pressure. A plant can regulate a cell's turgor pressure either

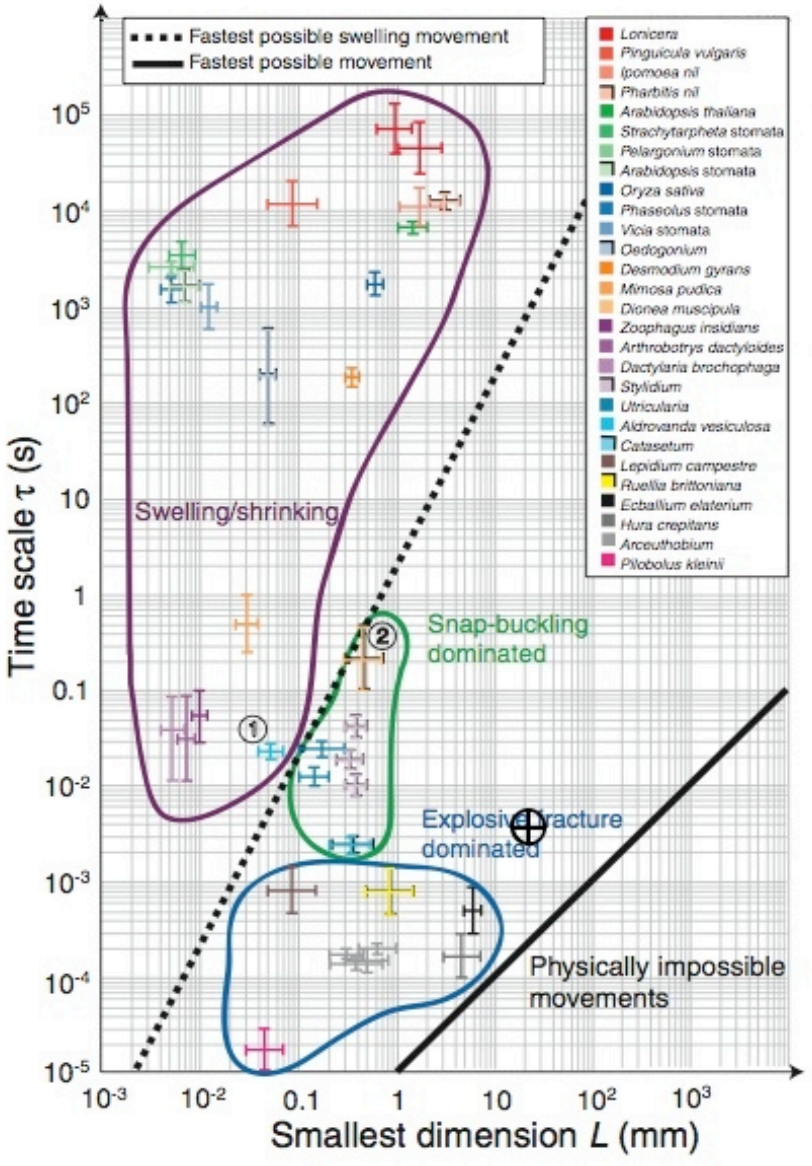

Figure 1.1: This graph shows known plant movements plotted as a function of time duration of movement τ and characteristic distance of fluid transport L. The dotted line marks the limit of movements that can occur by regulation of turgor pressure. To the right of the dotted line exist the movements that are generated by the release of stored elastic energy. *Impatiens pallida*, which has a characteristic distance L on the order of 20 mm and a time duration τ on the order of $4 \cdot 10^{-3}$ seconds, is marked on the graph by a circled cross. The solid line marks the limit of physically possible movements. Movements to the right of the solid line would require a propagation rate faster than the speed of sound, which is not possible. [16]

actively or passively. Drying is a form of passive regulation, while active regulation occurs when a plant controls the amount of fluid allowed in or out through the cell wall.

In both passive and active cases, the duration, τ, of these movements is constrained by the time it takes to transport fluid through a particular membrane and the characteristic distance, L, that the fluid is transported. Therefore, there is a lower limit to the time duration of hydraulic movements. This limit is called the poroelastic time, τ_p. Skotheim approximates the poroelastic time to be

$$\tau_p \sim \frac{\mu L^2}{kE} \tag{1.1}$$

where μ is the viscosity of the fluid, L is the characteristic length or distance of fluid transport, k is the hydraulic permeability of the membrane, and E is the elastic modulus of the membrane [16]. For plant tissue, a typical value of $\tau_p/L^2 = 1.6$ s/mm^2 [16]. Therefore, plant movements that are faster than this limit cannot be caused by regulation of turgor pressure. This boundary is represented by the dashed line in Skotheim's graph of plant movement as function of time duration τ and characteristic distance of fluid transport L seen as seen in figure 1.1. Movements with duration greater than the poroelastic time ($\tau > \tau_p$) are considered slow movements, and those whose duration is less than the poroelastic time ($\tau < \tau_p$) are classified as rapid movements [16].

Impatiens pallida has a characteristic distance of fluid transport L that is of the order of 20 mm and a time duration τ that is of the order of $4 \cdot 10^{-3}$ seconds. It therefore has a value of $\tau/L^2 \sim 10^{-5}$ s/mm^2. This is many orders of magnitude faster than the poroelastic time $\tau_p/L^2 = 1.6$ s/mm^2 meaning that the explosive seed dissemination of *I. pallida* classifies as a rapid plant movement.

The plant motions in the rapid-movement category are based on the release of stored elastic potential energy. Plant rapid movements have been found to have four distinct uses: (1) to disseminate seeds or sporangium; (2) for pollen emplacement; (3) for defense, and; (4) to obtain nutrition [16]. *Impatiens pallida* falls into the first group, it employs rapid movement to disseminates its seeds.

There are two sub-categories within the rapid movement category: the first is snap-buckling dominated, and, the second, explosive fracture dominated. The difference between the two is that snap-buckling involves a reversible change in the geometric shape of the plant, such as the closing of a trap of the Venus flytrap, *Dionaea muscipula*. This movement is a reversible process since *Dionaea muscipula* is

able to shut and open its traps going between two equillibrium position. Explosive fracture, the second category of rapid plant movement, involves the tearing of plant tissue, or dehiscence, in order to release stored elastic energy. It is an irreversible process and in general is the faster of the two movements.

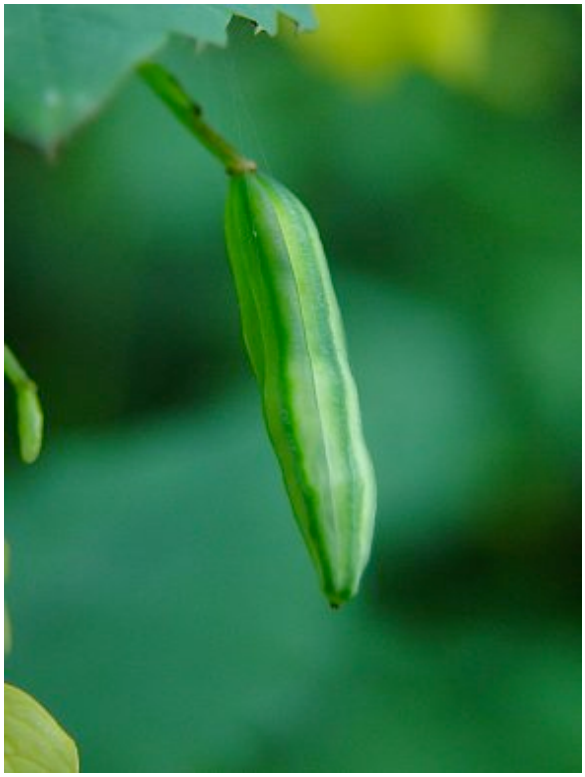

Figure 1.2: *Impatiens pallida* fruit [18]

The explosive seed dispersal of *Impatiens pallida* is categorized as an explosive-fractrure movement. *Impatiens pallida* fruit stores its elastic potential energy during its growth process. The fruit – a pod consisting of five valves encapsulating 3-4 seeds, which are held in place by the replum – takes approximately one month to reach maturity. During its growth process its valves develop such that the side closest to the seeds has a rest length much shorter that the side facing outwards (see figure 1.2). However since there is tissue holding the valves firmly in place, the outside segment of the valve develops under compression and the inside under tension such that both segments are of equal length. When the fruit dehisces or tears open, each valve separates from the others. Being no longer under stress, the outside and inside

of the valve return to their relaxed length thus releasing their stored elastic energy. When dehiscence is employed to disperse seeds, the process is called ballistochory.

Chapter 2

Impatiens

2.1 Introduction

Though the focus of this study is ballistochory in *Impatiens pallida*, the implications of our findings will shed light on the evolution of more than just this one species. The explosive propulsion of seeds is a feature shared by all *Impatiens* species. The explosive nature of the genus' fruit is what gives it its name. *Impatiens* is the Latin word for impatient, referring to the eager way in which it spreads its seed [8]. The fact that the *Impatiens* genus is exceedingly diverse, with species native to almost every continent, makes this common evolutionary trait even more interesting and significant subject of study. It is therefore important to have a general understanding of the genus as a whole.

2.2 The *Impatiens* Genus

The *Impatiens* genus is of the order Geraniales, in the family Balsaminaceae. It is characterized by wide diversity in terms of flower size, shape, and color, plant size, natural habitat, and native geographic location. The genus *Impatiens* has species native to almost every continent. *Impatiens pallida* is just one of more than one thousand of these species[8].

Impatiens species are endemic to temperate, subtropical and tropical parts of Africa, Madagascar, Asia (especially India), China and Southeast Asia, with a few species found in Europe and North America [8]. The only continents that cannot claim native species of *Impatiens* are Australia, South America and Antarctica [8]. *Impatiens* species are generally found to live in elevations between 1,000 and 3,000 meters and prefer climates that maintain temperatures below 25 Celsius. These plants

prefer living in damp shady environments, especially in areas near rivers or boggy ground [8]. However, they adapt well to sunny or shaded areas and grow easily in all except extremely dry conditions.

Even though *Impatiens* species tend to grow very well in other locations beside their native areas, it is not typical for a species to occur naturally in another location. Since *Impatiens* species prefer elevations between 1,000 and 3,000 meters and temperatures bellow 25 Celsius, the warmer climates of lower elevation act as a barrier preventing species naturally occurring in one location from traveling to another. Topographical changes such as landslides are the main cause for the initial isolation of a species. The warmer climate barrier keeps the isolated species from spreading to new areas, forcing it to evolve with its own particular characteristics. This phenomenon accounts for the wide diversity amongst the genus and the large number of independent species. This diversity is featured in the varied shape, size and color of *Impatiens* flowers as well as the wide variety of habitats in which they grow. Indeed *Impatiens* has among its species a spectrum reaching from lithophytes, plants that grow on bare rock, to semi-aquatic species that live in the middle of streams [8]. *Impatiens* also spans a wide range of plant height. *Impatiens glandulifera* grows to approximately 3 meters in height while the smallest *Impatiens* species grows to be only 8-10 high centimeters above the ground [8]. Despite its great diversity of species, all *Impatiens* use ballistochory as their form of seed dispersal.

The *Impatiens* fruit is a capsule with five identical elastic valves. The five sections are held together by tissue that rips during the launching process. A weak contact force such as slightly squeezing the pod will cause a ripe fruit to expel its contents. Inside the fruit there are 3-4 seeds held in place by the replum, a tissue that provides structure inside the fruit [2] (see Figure 2.2). Morgan divides *Impatiens* fruit into two cateogries based on their method of dehiscence. The two main groups are fusiform and linear [8]. *Impatiens* species with fusiform fruit are native to tropical areas while linear fruit are typical associated with species of temperate climates.

Fusiform fruit are shorter and rounder than the linear fruit. The method for dehiscence of the fusiform fruit is to open at the middle of the fruit and slit simultaneously out toward both ends. There is only one line of dehiscence and generally all five sections of the peel stay attached to each other after dehiscence.

Dehiscence for the linear fruit starts at the top end of the fruit, at the point where the fruit attaches to the plant. The rip then propagates longitudinally to the other extremity of the fruit. There are five lines of dehiscence resulting in each of the five valves separating from the rest but remaining attached at a single point at the bottom of the fruit. *I. pallida*, our plant of study, has this type of fruit.

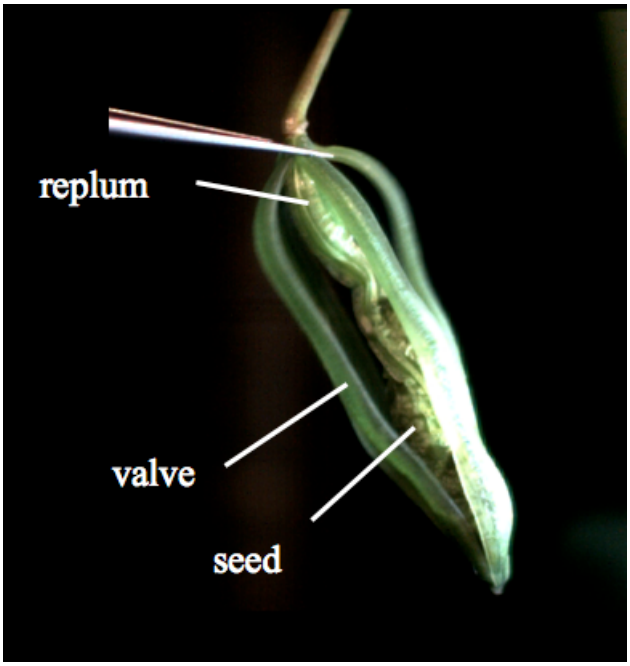

Figure 2.1: *Impatiens pallida* fruit during dehiscence from the video "pallida 9".

2.3 *Impatiens pallida*

There are two *Impatiens* species native to North America, *Impatiens capensis* and *Impatiens pallida*[8]. Both species are known commonly as jewelweed or touch-me-nots. The name jewelweed arises from the way spherical droplets of rain form on the plant and glisten in the sunlight. The droplets form perfect spheres because the *I. pallida* and *I. capensis* leaves repel moisture [1]. The name touch-me-nots of course comes from its exploding fruit.

Though both species are very similar, *Impatiens pallida* is slightly taller than *I. capensis*, has pale lemon-yellow flowers instead of orange spotted ones, and populates a smaller region than does *I. capensis* (see Figure 2.2 on page 9). *Impatiens pallida* occurs in the area limited by Nova Scotia, Saskatchewan, North Carolina and Missouri [12]. *Impatiens pallida* grows to be approximately 1-2 meters high and its foliage is dull grayish green [8].

Impatiens pallida's flowers, like all *Impatiens* flowers, are zygomorphic meaning that they have bilateral symmetry about only one axis. Bumblebees are pallidas

Figure 2.2: *Impatiens pallida* plant [18]

main pollinators and there have been six different species of *Bombus* recorded as the primary pollinators of the plant [4].

As previously mentioned, *Impatiens pallida*'s fruit falls into the linear category. The *I. pallida* fruit is a pod as seen in figure 1.2. We found the pods to have an average length of 2.6 ± 0.3 cm and an average width of 0.53 ± 0.05 cm. The *Impatiens pallida* fruit consists of five valves that make up the shell of the seedpod. These five valves distributed around the fruit in a radially symmetric configuration. Inside the shell are 3-5 seeds that rest end to end longitudinally in the pod. The seeds are held in place by the replum, a tissue that serves as support for the seeds. After pollination, its fruit takes about one month to reach maturity [1]. Once ripe, it can launch its seeds up to twelve feet in distance [21].

Chapter 3

Data Acquisition and Qualitative Analysis

3.1 Introduction

The motivation for studying ballistochory in *Impatiens pallida* comes from the knowledge that through evolution, plants develop mechanisms to ensure the continuation of their species. Therefore, given the many factors in play such as habitat, predators, pollinators, climate and elevation, ballisochory must be the best possible means of for *I. pallida* to propagate. There are many insights to be gained from understanding this key developmental feature. For a plant like *Impatiens pallida*, understanding its intrinsic seed launching mechanism gives us deeper insight into the plant's evolutionary history and will help biologist answer many questions such as: What is its purpose of developing a seed launching mechanism, and what is the plant achieving in doing so? Is it trying to avoid predators? If so, which predators is it successful in avoiding? Which predators trigger its mechanism? How does it want its seeds spread? How much mass needs to be contained in a seed for it to serve its purpose? What is the plant trying to maximize: projectile distance, mass of the seed, or some other quantity? This study will also serve as a model for the study of ballistochory in the other 1000 *Impatiens* species.

3.2 Data Collection: High-Speed Photography

Our first step in this study will be to investigate the mechanics of *I. pallida*'s launch process. Though plant movement has been studied for some time now, little research has been done on ultra-rapid plant movement such as this one. The biggest

obstacle being that we lacked the technology to view the process in detail. High-speed photography has proved to be the essential tool necessary for the study of movements such as *I. pallida*'s seed lauch that are just a few milliseconds in duration. High-speed photography has given us a way to zoom in, with better and better resolution, to events that occur in time in the same way that microscopes have provided a way for us to view, with better and better resolution, in the spatial dimension. We therefore used high-speed photography to record the fruits explosion and video analysis software to analyze the biomechanics at work.

The camera used to record the launch processes was a Redlake HG-100K, a high-speed digital camera. This video camera is able to take up to 100,000 frames per second–unlike regular video cameras which record 30 frames per second. To take images in this type of photography the object being filmed needs to be extremely well lit.

An interesting feature of the Redlake HG-100K it is triggered after the event being filmed occurs. The camera films continuously, and at any given moment only stores the images corresponding to the previous 5 seconds. When the camera is triggered it stops discarding images older than 5 seconds and permanently saves the 5 seconds of images it has on hand. This is an extremely useful feature when recording events whose occurrence cannot be predicted. For example, if instead of forcing *I. pallida*'s fruit to explode, we wanted to wait for it to explode on its own and record the process, it would be very inconvenient to turn on the video camera and wait for the event. This would waste storage space, even waiting 30 seconds would mean hundreds of thousands of useless images. The post-event trigger lets one wait to activate the camera until after the event occurs, helping us keep only the images we need.

The filming process went as follows: In the summer of 2005, sample fruit were taken from plants near Williamstown to a lab in Williams College where they were squeezed with a pair of tweezers and their explosions were filmed. Using this method, Professors Dwight Whitaker of Pomona College and Joan Edwards of Williams College recorded a total of 24 videos. Of the 24 videos taken, 17 were recorded with a frame rate of 5,000 frames per second and seven with a frame rate of 2,000 frames per second. In most of the trials the fruit was triggered by exerting pressure with a pair of tweezers at the top of fruit. However, there were some trials where the fruit was squeezed at different locations along its length to investigate the seedpod's process of dehiscence. Twenty of the videos were triggered by squeezing at the top of the fruit, two at the bottom, one in the middle and one at a quarter of the length from the top of the fruit.

3.3 Qualitative Analysis of Dehiscence

In December of 2007 we began our video analysis. From the videos we learned several important facts about the dehiscence process. Dehiscence always begins at the top of the fruit, at the place where the fruit attaches to the rest of the plant. The rip then propagates longitudinally downward to the other end of the fruit. We tried triggering the pod at different points, but regardless of whether it is squeezed at the middle or either end, the rip always started at top.

This discovery is significant for several reasons. 1.) Since the fruit detaches completely from the plant at the initial stage of dehiscence, we know there are no outside forces acting on the fruit nor is the fruit acting on the plant during the seed launching process. This means we can consider the fruit a closed system during the launch process where all forces are internal and total energy is conserved. 2.) The plant's choice to initiate dehiscence by detaching the fruit from the branch greatly increases the seed's projectile distance.

It is clear that if dehiscence began and the bottom and propagated upwards the projectile distance would be reduced since the the initial direction of the seed's velocity would be downward. Also, if dehiscence began at the bottom of the fruit, the peel would not be able to detach itself from the branch of the plant. The pod would be forced to expend its energy moving the mass of the branch as well as the seeds, reducing the amount of energy transfered to the seeds. Figure 3.1 simulates how difficult it would be for the fruit to launch its seeds while remaining attached to the plant. In "pallida 8 we pretend the tweezers are an extremely massive fruit branch, thus dehiscence starts at the point furthest from the 'branch' and propagates toward it. "Pallida 7" shows the regular process of dehiscence. When we compare the two processes we notice that after 0.010 s "pallida 7"'s seeds are traveling away from the branch whereas "pallida 8"'s seeds remain hovering around the fruit and have not traveled.

Another interesting quality we observed is that after causing the fruit to detach from the plant, the rip then propagates down the length of the pod separating each valve from its neighbors. As the valves separate from each other they begin to curl inwardly while simultaneously rotating away from the longitudinal axis of the fruit. This means that each valve is contributing momentum to the seeds and replum in two ways. 1.) Through conservation of momentum: As the valves rotate away from the fruit's centra axis they are redistributing the mass in the system. The seeds and replum will then be forced upwards in order to keep the center of mass of the fruit from shifting. 2.)Through the restorative elastic force contributed by each valve to the bottom of the replum.

Figure 3.1: The first 10 ms of the ballistochoric process of "pallida 7" and "pallida 8". "Pallida 7" is triggered from the top of the fruit and we see the seeds projected away from the plant. For "pallida 8", the pinch that triggers dehiscence also holds the fruit's peel in place making it unable to catapult the seeds.

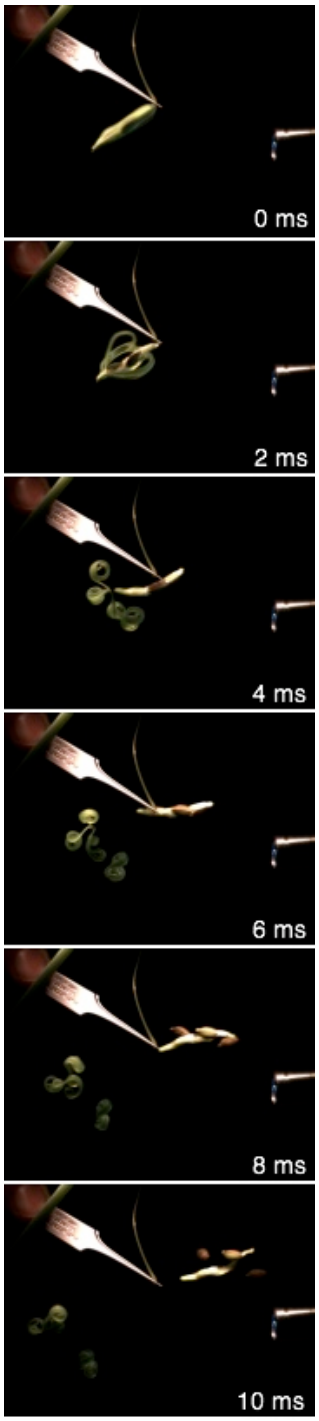

(a) "pallida 7"

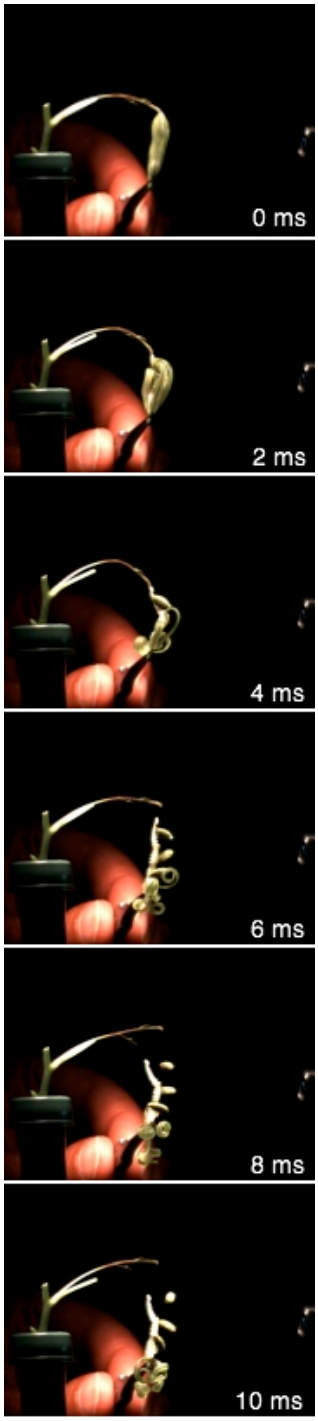

(b) "pallida 8"

The fact that the valves curl inward is key to the propulsion of the seeds. If the valves curled outward instead, then the elastic force of the valve would point away from the replum instead of towards it as modeled in figure 3.2. The blue arrow represents the elastic force of one valve. When the valves curl inward the lateral component of their elastic forces cancel out leaving only the component pointing along the axis of the replum. When the valves curl inward this resulting force is pointing upwards, towards the replum and that is why the seeds and replum are launched away. If the valves curled in the opposite direction, then the resulting force would be directed downward, away from the replum and the valves would pull the replum down. Thus, in this scenario, the elastic force of the valves would not contribute to the seeds' projection. Conservation of momentum, however, would still act to propel them upwards.

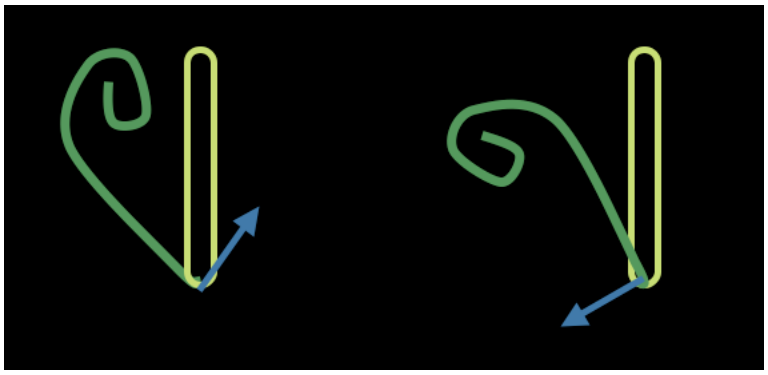

Figure 3.2: This figure depicts the elastic force contributed by a valve to the replum. The example on the left acurately depicts the direction of curling of *Impatiens pallida* valves. The blue arrow describes the direction of the elastic force. The right hand drawing exemplifies what would happen if the valves curled outwardly instead of inwardly. We see that the elastic force would point away from replum.

Chapter 4

Data Reduction

4.1 Introduction

After noting the key features of the dehiscence process, we were motivated to begin a quantitative analysis of the seed-launching mechanism. Our goal here is to provide the data necessary to create a theoretical model of the fruit's explosion and to learn more about the dehiscence process. Since the fruit is a closed system, we can study the internal forces that result in the seeds' projection by studying the motion of the different components over time. If our data is ultimately used to create the theoretical model it is imperative that it be as accurate as possible. Since the theoretical model would be a model of the fruit's internal forces, we must eliminate from our data all effects of outside forces. Also, from the reduced position versus time data for the seeds, replum, and valves, we can compute the components' velocities and accelerations. Once we know the final velocities of all components we can calculate the total final kinetic energy of the system. By conservation of energy, this value will provide us with a lower bound for the quantity of stored elastic energy that was released during dehiscence.

4.2 Video Analysis

We began our quantitative analysis with a frame-by-frame study of the evolution of the launch process. We used LoggerPro's video analysis software. LoggerPro allows the user to mark a point on each frame of a video. The software then created a table correlating the x and y coordinates of the marked point to its corresponding frame. One unfortunate feature of this software is that it allows the user to follow only three objects per file. Therefore, to trace the fruit's nine components – five valves of the peel, three seeds and, the replum – we had to use multiple files increasing our margin

of error.

We estimated the center of mass of the seeds by locating the center of the seed's visible shape. In the earlier frames, when the seeds are still concealed by the peel and not observable, we would run through the slides in reverse order several times in order to get a sense of the seed's location before marking its center of mass. For the replum, we marked its midpoint as its center of mass, repeating the above procedure to estimate its location while it was still inside the peel. The valves of the peel presented the biggest challenge. When they are straight we mark their center of mass as the point halfway down their length. Once they began to curl we placed the center of mass on the the concave side of the peel, estimating there to be the same amount of mass above as bellow the point as well as to the left and right of it. In figure 4.1(a), the lone blue dot is our latest estimate for leftmost valve's center of mass. Figure 4.1(b) shows the estimate for the center of mass of the valve once it has curled completely.

We chose "pallida 7" as the main video of study because it provided the longest view of the components' trajectories and because neither the seeds nor the replum hit the tweezers during the process. For simplicity, we divided the fruit's components into two systems. The five valves of the peel make one system and the seeds and replum make another. After the fruit explodes, these systems are moving in opposite directions. Our next step was to find the center of mass for each of these two systems.

To find the center of mass of each system we need to know the individual masses of each component in the system. Though we did not record the mass of "pallida 7" we did have mass data for 15 other fruit. We took the total seed mass for each fruit and divided it by the number of seeds present to find the average mass of each seed, we then found the average mass of a seed across all 15 fruit. We calculated the average mass of a seed to be 0.024 ± 0.007 g. Similarly we found the average mass of a peel valve was 0.033 ± 0.008 g and the average mass of the replum 0.033 ± 0.006 g.

From the mass and position data of each of the components we calculated the x and y coordinates of the center of mass of each system using the following equations:

$$x_{CM} = \frac{\sum_{i=1}^{n} m_i x_i}{\sum_{i=1}^{n} m_i} \qquad y_{CM} = \frac{\sum_{i=1}^{n} m_i y_i}{\sum_{i=1}^{n} m_i} \tag{4.1}$$

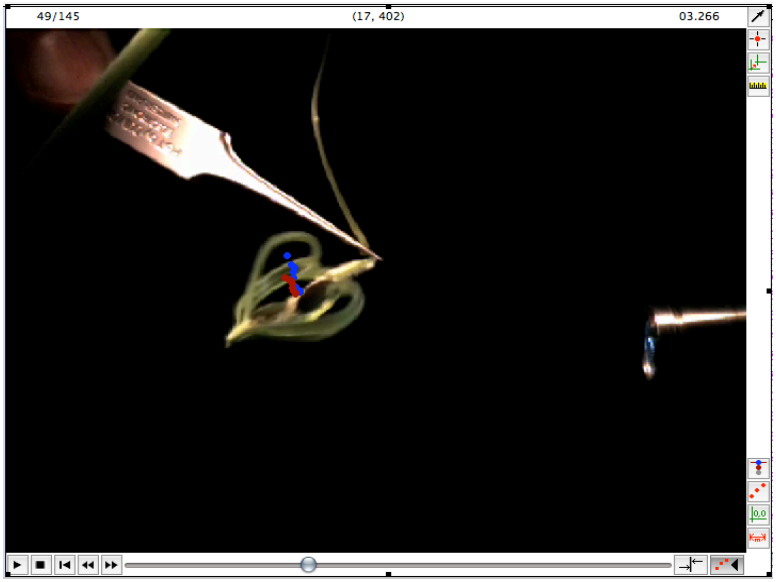

(a) After 11 frames.

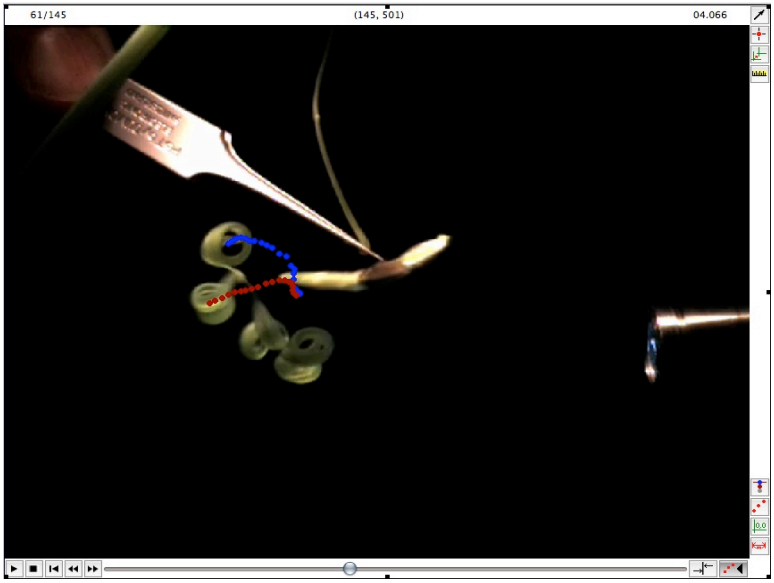

(b) After 23 frames.

Figure 4.1: Images of LoggerPro file for the video "pallida 7". Here we are tracing the center of mass of two of the peel's valves.

where m is mass, x and y are position and, i denotes each of the components in the system.

Similarly we found the center of mass of the fruit as a whole. We expected fruit's center of mass to remain motionless during the launch process since it is a closed system. However, when we plotted the x versus y position of the center of mass (see figure 4.2) we saw its position was moving in time. One explanation for the motion of center of mass is that the force of gravity has acted upon the fruit and displaced it's center of mass according to the equation

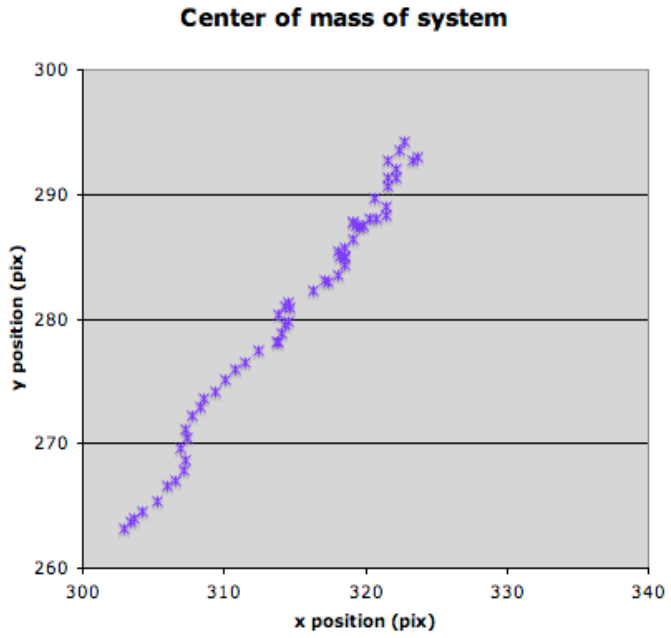

Figure 4.2: Plot of center of mass of the entire fruit system with x-position on the x-axis and y-position on the y-axis. Each mark represents a frame of the video and thus show the center of mass' trajectory over time. This plot shows that the center of mass of the system is moving at a constant velocity. We assume that its motion originated from an impulse given to the system by the tweezers when it was triggered.

$$y(t) = -gt^2 + v_{oy}t + y_o \tag{4.2}$$

If we assume that the fruit has no initial velocity, therefore, $v_{oy} = 0$ and $y_o = 0$, its y displacement due to gravity must be $y(t) = -gt^2$. Since the duration of the

explosion is less than 0.012 s we see that the displacement in the y-direction due to effects of gravity would be approximately 1.4 mm or about 8 pixels. However, in figure 4.2 we see that the displacement is on the order of 30 pixels so gravity could not have accounted for all of it. Also, the force of gravity would only account for the displacement in the y-direction and not in the x-direction. For these reasons we discarded the force of gravity as the only cause for the displacement of the system's center of mass.

This realization lead us to suspect the motion of the center of mass was caused by an outside force. It is likely that we gave the fruit an initial impulse when we squeezed it with the tweezers. In order to study the internal forces of the fruit system we needed to eliminate the motion caused by an outside force from our data. We achieved this by transfering our data into the reference frame of the center of mass. In this reference frame, the center of mass of the system is at rest and the motion of the system's components is due sole to internal forces. We corrected our data by preforming the Galilean transformation

$$\begin{aligned} x'(t) &= x(t) - v_{CM_x} t \\ y'(t) &= y(t) - v_{CM_y} t \end{aligned} \tag{4.3}$$

where primed frame is the frame where the fruit's center of mass is at rest. In the above equations, v_{CM_x} and v_{CM_y} are the x and y components of velocity for the system's center of mass. We computed these velocities by finding the slope of the x position data and y position data respectively. Figure 4.3 shows the x and y positions of the center of mass in the primed frame. We see that in the primed frame, the center of mass of the system is confined to one general location. We also notice that the position of the eight initial frames lies outside this region. This is due to the error in estimating the center of mass of each component especially of the seeds during the initial stages of dehiscence. During these stages the seeds are still hidden from view and we had to estimate their location and center of mass. The data for the center of mass is likely to become more accurate after the ninth frame, once the seeds became visible in the video.

We next preformed the Galilean transformation on the position data for the center of mass of the seeds, replum, and peel. Figure 4.4 shows the x and y positions of the seeds and replum and the peel over time in the primed frame. We can see that there is a period of acceleration and that after 0.003 s both systems are moving at a constant velocity.

In the primed frame we see that the peel system and the seeds and replum system have both x and y components to their velocity. However, it is clear to us from the

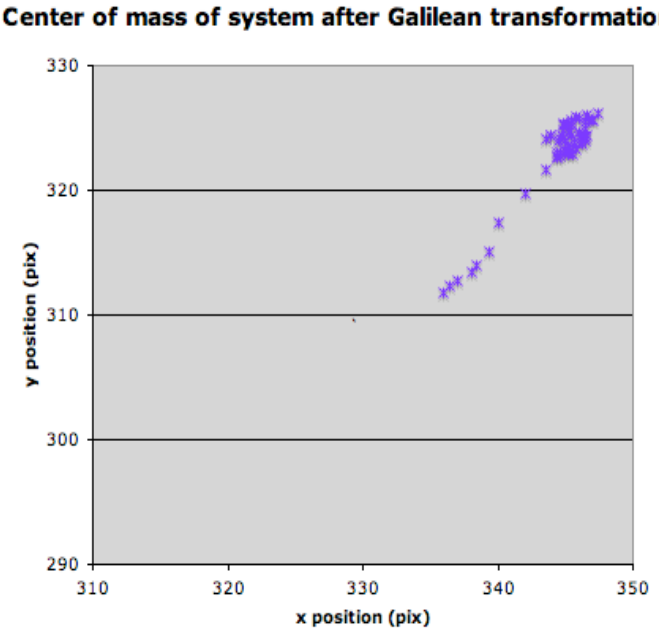

Figure 4.3: Plot of center of mass of the system after preforming the Galilean transformation. X-position is on the x-axis and y-position on the y-axis. Each mark represents a frame of the video and thus show the center of mass' trajectory over time. This plot shows the center of mass is at rest during the process.

videos that there exists a coordinate system in which the motion of both systems would be in only one dimension; a reference frame in which its velocity would be entirely along one axis.

Our next step was to rotate our coordinate axes to capitalize on the symmetry of the system. To do this we needed to find the angle, θ, by which to rotate the reference frame (see figure 4.5). Since we know the x and y components of the velocity of the peel system and of the seeds and replum system we can find θ by solving

$$\frac{v_y}{v_x} = \frac{v \sin\theta}{v \cos\theta} = \tan\theta \tag{4.4}$$

Therefore,

$$\arctan\left(\frac{v_y}{v_x}\right) = \theta \tag{4.5}$$

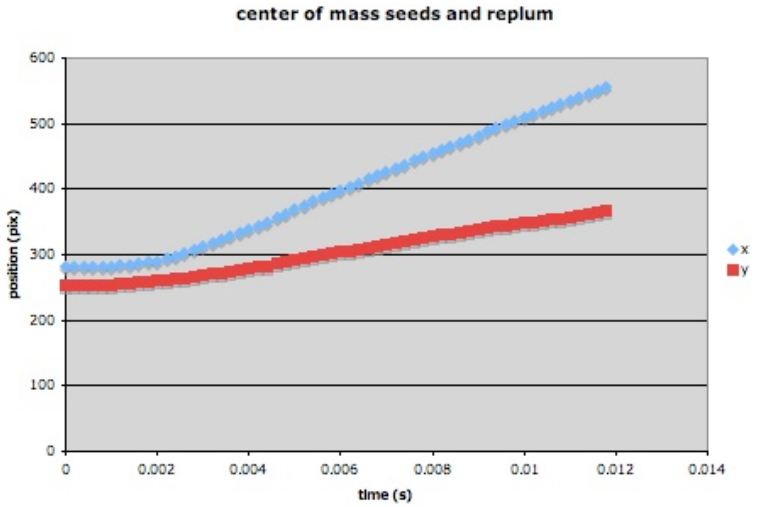

(a) Center of mass of seeds and replum

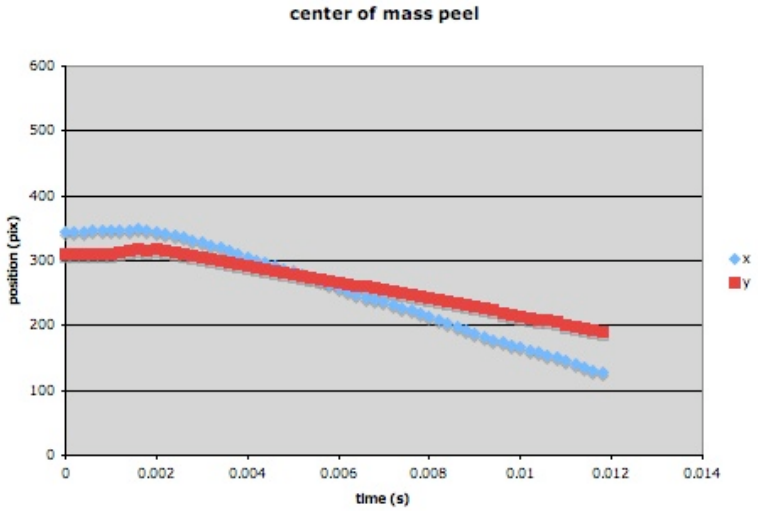

(b) Center of mass of peel

Figure 4.4: This figure shows the x and y coordinates of the center of mass of the peel and the center of mass of the seeds and replum system in the primed frame where the center of mass of the entire system is at rest.

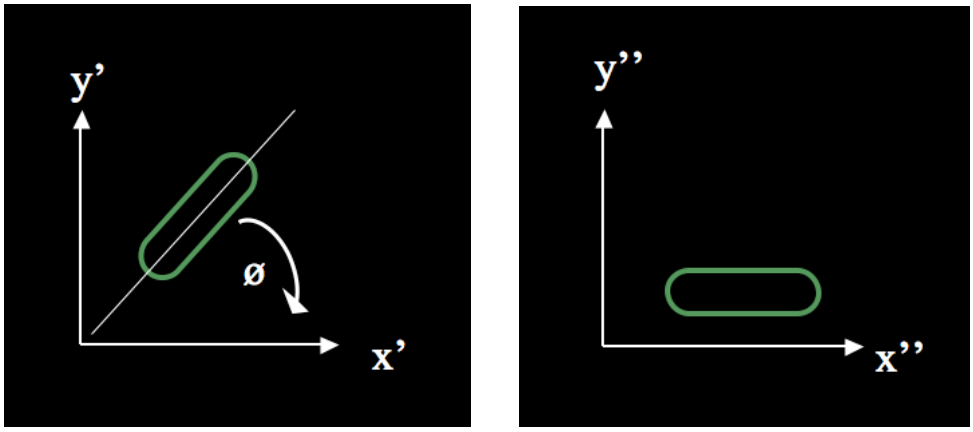

(a) Reference frame before rotation. (b) Reference frame after rotation.

Figure 4.5: We rotated our frame of reference by angle θ in order to take advantage of the fact that the motion of the fruit lies in one dimension.

We calculated θ for the peel system and the seeds and replum system and averaged both values to get $\theta = 25.6°$. We then used the following rotation matrix

$$\begin{bmatrix} x'' \\ y'' \end{bmatrix} = \begin{bmatrix} \cos\theta & -\sin\theta \\ \sin\theta & \cos\theta \end{bmatrix} \begin{bmatrix} x' \\ y' \end{bmatrix} \tag{4.6}$$

and our value of theta to translate our x and y position data to the double-primed frame where all motion would be in the x-direction. As seen in figure 4.6 the y-position of both the seeds and replum and the peel are not changing in time.

We then used the x-position of the systems in the rotated frame to find the velocity of the peel and the velocity of the seeds and replum. We calculated the instantaneous velocity between each frame using the equation

$$v_x = \frac{x_{n+1} - x_n}{\Delta t} \qquad v_y = \frac{y_{n+1} - y_n}{\Delta t} \tag{4.7}$$

where n refers to the frame number, and the time step Δt depends on the frame rate at which the video was taken. For "pallida 7", which was taken at 5,000 frames per second, Δt is 0.0002 s.

We then took the slope of the linear part of of the velocity data to find an average velocity for each the peel and the seeds and replum. The linear part of the data begins after the replum detaches from the peel, and is therefore final velocity for

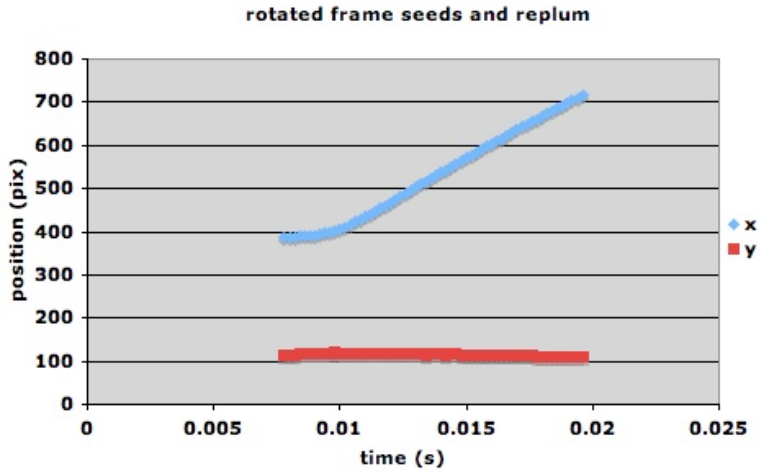

(a) Center of mass of seeds and replum in the rotated frame

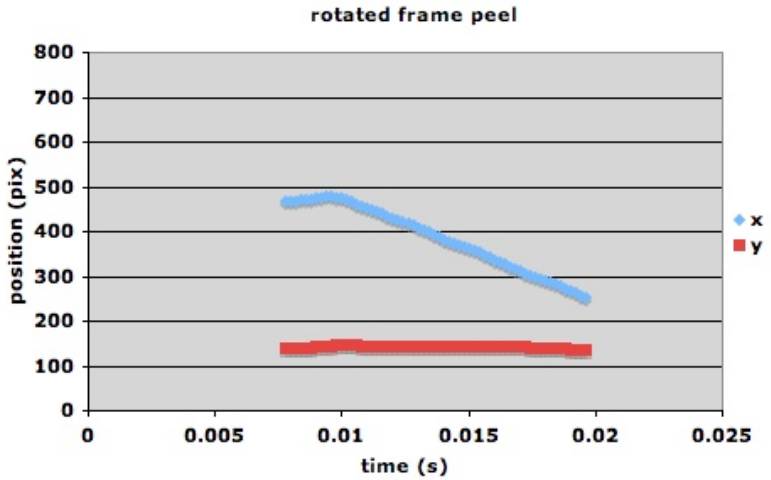

(b) Center of mass of peel in the rotated frame

Figure 4.6: This figure shows the x and y coordinates of the CM of the peel system and the CM of the seeds and replum system the double-primed frame. Here the coordinate axes have been rotated so that all motion is in one dimension. We can see that the y position of both systems is static over time

each component. The peel had a final x velocity v_x of -4.08 ± 0.54 m/s and v_y of -0.13 ± 0.31 m/s. We calculated v_x for the seeds and replum to be 5.76 ±0.62 m/s and v_y to be -0.14 ± 0.27 m/s. In both systems we see that the y component of the velocity is within the uncertainty of being zero.

From these velocities and our estimated masses we calculated the total translational kinetic energy of all sections of the fruit at the end of the explosion. The total translational kinetic energy of "pallida 7" was 0.0031 J.

Chapter 5

Quantitative Findings

5.1 Introduction

As noted previously, the fact that dehiscence begins at the top of the fruit means we can consider the fruit a closed system, which conserves energy. We can assume the total amount of energy released in the fruit's explosion is equal to the amount of energy stored in the valves of the peel in the form of strain energy. In the previous chapter we calculated the total final kinetic energy of the fruit. This value is the lower limit of the elastic energy or strain energy initially stored in *I. pallida*'s fruit valves. Since we are not including rotational kinetic energy nor accounting for every other form of energy dissipation, we know translational kinetic energy is the least amount of energy released in the explosion. From this estimate for strain energy we can calculate the elastic modulus or Young's modulus E of the fruit's valves. Young's modulus is a material property, it is a measure of stiffness which is equivalent to a spring's spring constant.

5.2 Strain Energy

We used continuum mechanics to derive a formula for the strain energy stored in each valve as a function of its thickness, height, length, radius of curvature, and Young's modulus. From this equation we estimated Young's modulus. However, since our value of strain energy is the lower limit of the energy possibly stored in the peel, our estimate is a lower bound of Young's modulus.

We will model each valve as a beam with an initial radius of curvature ρ where ρ is the distance from the neutral axis of the beam to the center of curvature O (see figure 5.1). The neutral axis, represented by the solid line inside the beam in figures

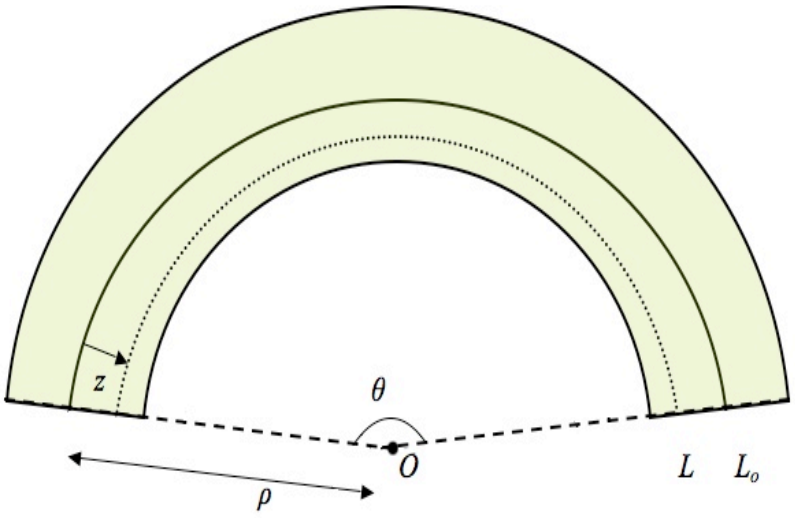

(a) Beam in its relaxed state.

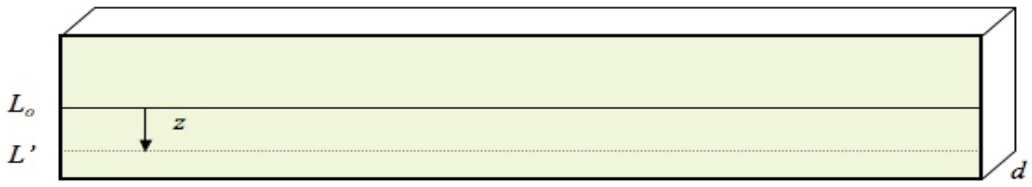

(b) Beam under stress.

Figure 5.1: To derive an equation for the strain energy stored in the peel of *I. pallida*'s fruit we will consider each valve as a beam. This beam is initially under stress but then returns to its relaxed state by releasing its stored elastic energy.

5.1(a) and 5.1(b), is defined as the segment in the beam that does not change in length during beam deflection. Lets the length of this segment be L_o, where

$$L_o = \rho\theta \tag{5.1}$$

Let us also consider a segment L, the dotted line in figures 5.1(a) and 5.1(b), located at a distance z below the neutral axis. Initially,

$$L = (\rho - z)\theta \tag{5.2}$$

Let us now consider the case where we take this initially curved beam and apply a force such that we reduce its curvature until it becomes essentially straight. Now all segments above the neutral axis are under compression, or negative strain, and all segments below the neutral axis are under positive strain. All segments are now equal to L_o. To calculate the change in length δ of our segment L we must compute

$$\delta = L - L_o \tag{5.3}$$

to get

$$\delta = (\rho - z)\theta - \rho\theta = -z\theta \tag{5.4}$$

We can then find strain ϵ by calculating change in length over original length for our segment L,

$$\epsilon \equiv \frac{\delta}{L} = \frac{-z\theta}{(\rho - z)\theta} = \frac{-z}{(\rho - z)} \tag{5.5}$$

The next step is to find the stress σ of our line segment. By definition, stress σ is related to strain ϵ by Young's modulus E. Hook's law gives the equation

$$\sigma = E\epsilon \tag{5.6}$$

The stress σ in a beam is also equivalent to the amount of force F applied to the beam divided by the beam's cross-sectional area A. In our case, the cross-sectional area of our line segment L is an infinitesimal area dA where

$$dA = dz \cdot d \tag{5.7}$$

where d is the depth or width of the beam. Therefore, stress σ can also be expressed as

$$\sigma = \frac{F}{dA} = \frac{F}{dz \cdot d} \tag{5.8}$$

Equating equations 5.6 and 5.8 and solving for force F we observe

$$F = E\epsilon d \cdot dz \tag{5.9}$$

Plugging in equation 5.5 for strain ϵ in equation 5.9 we see that

$$dF = \frac{-zEd}{(\rho - z)}dz \tag{5.10}$$

This is the infinitesimal amount of force needed to stretch or compress a segment of the beam with length L, height dz and, depth d which lies at a distance z from the neutral axis.

Next we will find the infinitesimal amount of work dW done to a segment of the beam to stretch or compress it by a distance δ. Since work is equal to the amount of force F times the distance it is applied over, we can compute

$$dW = dF \cdot \delta \tag{5.11}$$

as the amount of work done on one segment of the beam. If we substitute equation 5.10 for dF and 5.4 for δ we obtain

$$dW = dF \cdot \delta = \frac{z^2 E\theta d}{(\rho - z)}dz\cdot \tag{5.12}$$

We can also substitute L_o/ρ for θ to obtain

$$dW = dF \cdot \delta = \frac{z^2 EL_o d}{\rho(\rho - z)}dz \tag{5.13}$$

Lastly, to find the total amount of work done to deflect the entire beam we simply integrate dW over z from a value $-h$ to h, where h is half the height of the beam. Our integral would take the form

$$\int dW = \int_{-h}^{h} \frac{z^2 EL_o d}{\rho(\rho - z)}dz \tag{5.14}$$

In the limiting case where ρ is greater that z the total amount of work done on the beam is

$$W = \frac{2EL_o d \cdot h^3}{3\rho^2} \tag{5.15}$$

which can also be expressed in terms of the volume V of the beam as

$$W = \frac{EV \cdot z^2}{3\rho^2} \tag{5.16}$$

This equation shows us that the work done goes as $1/\rho^2$ meaning the smaller the radius of curvature, the more work done. It also goes as z^2 which expresses that the taller the beam is in the direction of bending the more work it takes to deflect it.

Since the amount of work done to deflect the beam is equal to the strain energy stored in the beam, we can assume equations 5.15 and 5.16 express the elastic potential energy stored in each of the fruit's valves. If we multiply this value by five to account for the five valves we will have an expression for the total strain energy of the fruit. Here we will equate potential energy to the kinetic energy T of the fruit's components after dehiscence. We can therefore solve equation 5.16 to get an expression for Young's modulus

$$E = \frac{3T\rho^2}{5Vh^2} = \frac{3T\rho^2}{10L_o d \cdot h^3} \tag{5.17}$$

Using this equation and the value for kinetic energy T derived in chapter 4 we calculated a preliminary estimate of Young's modulus E. We used the program ImageJ to measure the thickness $2h$, radius rho, length L_o and depth d of the valves of "pallida 7". Using the 'measure' tool on ImageJ and the known width of the flashlight that appears in the video "pallida 7" we measured the pixel to centimeter ratio of the images to be 57 pix/cm. With this same tool we measured the pod's length L_o to be 2.7 cm and the valve depth d to be 0.31 cm. The valve's $2h$ was 0.17 cm. We measured the valve's radius of curvature in two ways and got similar answers. First we used the 'measure' tool to find the valves diameter, being careful to measure to half the thickness of the valve since ρ is the distance from the center of curvature to the neutral axis. Our second technique was to draw a circle on top of the valve and use ImageJ's 'measure' tool to calculate its area. We then divided by π and took the square root to find ρ. Both techniques gave us an approximate value of 0.31 cm.

Plugging these values into equation 5.17 produced an value of Young's modulus on the order of 0.1 MPa. This value was many orders of magnitude lower than expected.

Stretch tests done on leaves of the *Quercus* or Oak genus measured the leave to have a Young's modulus ranging from 5-20 MPa[13]. A human tendon has a significantly higher modulus of 2 GPa. We expected the valves of the *Impatiens* fruit to have a stiffness within this range predicting that its value of Young's modulus would be closer to that of a human tendon than a leaf.

Before beginning this calculation we knew our estimate would be a lower bound on Young's modulus, since we were only accounting for translational kinetic energy. However, it seems there may be other reasons why our value low. It is possible that we overestimated the value of the valve's thickness $2h$. The valves are longitudinally concave. Thus from a side view like the one we have in our video, one can overestimate its thickness. Through further study and investigation we will discover more explanations and find a more accurate value for the Young's modulus of *Impatiens pallida* valves.

Chapter 6

Conclusion

In this research, we successfully unclouded the mechanisms employed by the plant *Impatiens pallida* to expel and disseminate its seeds. Though the use of high-speed filmography, video analysis software, and the employment of physical principals we were able to produce qualitative results for the velocity, acceleration and translational kinetic energy, of the components of *I. pallida*'s fruit.

High-speed filmography enabled us to view important qualitative features of *I. pallida*'s dehiscence. For example, we observed how the dehiscence process always began at the point where the fruit attaches to the branch making it possible for the fruit to release itself from the plant in order to expend its energy launching the seeds. We also noted that the valves curl inwards exerting an elastic force that propels the seeds and replum. Simultaneously, the valves rotate away from the replum forcing it to move upwards to conserve momentum. We measured the velocity of the ballistic seeds to be on the order of 6 m/s by reducing our data until all motion was in a single dimension. We also computed a preliminary value of the Young's modulus of the fruit's valves by employing continuum mechanics.

This undergraduate thesis has provided the groundwork for the development of a physical model of ballistochory in *Impatiens pallida*. Our reduced data provides the foundation on which we can develop and evaluate the usefulness of a specific theoretical model.

Another success lies in the development of tool the study and analysis of plant movement. The tools we created to study *Impatiens pallida* include the use of high-speed filmography to uncover qualitative models of dehiscence as well as methods for data reduction. Our results also provide insights for biologist who are seeking to understand plant dehiscence and more specifically, ballistochory in the vast *Impatiens* genus.

Bibliography

[1] Adams, Kevin, and Marty Casstevens, eds. 1996. Wildflowers of the southern appalachians: How to photograph and identify them. Winston-Salem, N.C.: J. F. Blair.

[2] Blanchan, Neltje, and Asa Don Dickinson, eds. 1923. Wild Flowers Worth Knowing . Adapted by Asa Don Dickinson from Nature's Garden, by Neltje Blanchan Pseud. Garden City, New York, Doubleday. XVIII, 270 P., Illus. (Part in col.) 21 CM: .

[3] Forterre, Y., et al. "How the Venus Flytrap Snaps." Nature 433.7024 (2005): 421-5.

[4] Frey, F. M., R. Davis, and L. F. Delph. 2005. Manipulation of floral symmetry does not affect seed production in impatiens pallida. International Journal of Plant Sciences 166, (4) (JUL): 659-62.

[5] Garrison, W. J., G. L. Miller, and R. Raspet. "Ballistic Seed Projection in Two Herbaceous Species." American Journal of Botany 87.9 (2000): 1257-64.

[6] Gere, James M., and Stephen Timoshenko, eds. Mechanics of Materials. 2nd ed. Monterey, Calif.: Brooks/Cole Engineering Division, 1984.

[7] Landau, L. D., et al, eds. Teoriia Uprugosti English; Theory of Elasticity. 3rd English , revis and enlarg by E.M. Lifshitz, A.M. Kosevich, and L.P. Pitaevskii ed. Oxford Oxfordshire ; New York: Pergamon Press, 1986.

[8] Morgan, Raymond J. 2007. Impatiens : The vibrant world of busy lizzies, balsams, and touch-me-nots. Portland, Or.: Timber Press.

[9] Nozzolillo, C., and I. Thie. "Aspects of Germination of Impatiens-Capensis Meerb Formae Capensis and Immaculata, and Impatiens-Pallida Nutt." Bulletin of the Torrey Botanical Club 110.3 (1983): 335-44.

[10] Popov,E P (Egor Paul),. Introduction to Mechanics of Solids Egor P Popov. Englewood Cliffs, N.J.,: Prentice-Hall, 1968.

[11] Pringle, A., et al. "The Captured Launch of a Ballistospore." Mycologia 97.4 (2005): 866-71.

[12] Rust, R. W. 1977. Pollination in impatiens-capensis and impatiens-pallida-(balsaminaceae). Bulletin of the Torrey Botanical Club 104, (4): 361-7.

[13] Saito, Takami, et al. "The Bulk Elastic Modulus and the Reversible Properties of Cell Walls in Developing Quercus Leaves." Plant and Cell Physiology 47.6 (2006): 715-25.

[14] Schmitt, Johanna, David Ehrhardt, and Daniel Swartz. "Differential Dispersal of Self-Fertilized and Outcrossed Progeny in Jewelweed (Impatiens Capensis)." The American Naturalist 126.4 (1985): 570-5.

[15] Simons, Paul. The Action Plant : Movement and Nervous Behaviour in Plants. Oxford, UK ; Cambridge, Mass., USA: Blackwell, 1992.

[16] Skotheim, J. M., and L. Mahadevan. "Physical Limits and Design Principles for Plant and Fungal Movements." Science 308.5726 (2005): 1308-10.

[17] Stamp, N. E., and J. R. Lucas. "Ecological Correlates of Explosive Seed Dispersal." Oecologia (Berlin) 59.2-3 (1983): 272-8.

[18] Tenaglia, Dan. Impatiens Pallida Nutt. - Yellow Touch-Me-Not. 2003. Ozark Scenic Riverways, Shannon County, MO. Missouri Flora Web Page. $< http : //www.missouriplants.com/Yellowalt/Impatiens_pallida_page.html >$.

[19] Timoshenko, Stephen1972, and D. H. jt auth Young, eds. Elements of Strength of Materials [by] S Timoshenko and D H Young. 4th ed. Princeton, N.J.,: Van Nostrand, 1962.

[20] Whitaker, D. L., L. A. Webster, and J. Edwards. "The Biomechanics of Cornus Canadensis Stamens are Ideal for Catapulting Pollen Vertically." Functional Ecology 21.2 (2007): 219-25

[21] Whitaker, Dwight L. Mar. 2008. Personal communication.

[22] Witztum, A., and K. Schulgasser. "The Mechanics of Seed Expulsion in Acanthaceae." Journal of theoretical biology 176.4 (1995): 531-42.